2017

Gene expression profiling of bovine ovarian follicular and luteal cells provides insight into cellular identities and functions

Sarah Romereim
University of Nebraska-Lincoln, sromereim2@unl.edu

Adam F. Summers
University of Nebraska - Lincoln

William E. Pohlmeier
University of Nebraska - Lincoln

Pan Zhang
University of Nebraska Medical Center, pan.zhang@unmc.edu

Xiaoying Hou
University of Nebraska Medical Center, xhou@unmc.edu

See next page for additional authors

HHS Public Access

Author manuscript

Mol Cell Endocrinol. Author manuscript; available in PMC 2019 August 27.

Published in final edited form as:

Mol Cell Endocrinol. 2017 January 05; 439: 379–394. doi:10.1016/j.mce.2016.09.029.

Gene expression profiling of bovine ovarian follicular and luteal cells provides insight into cellular identities and functions

Sarah M. Romereim[a], **Adam F. Summers**[a,1], **William E. Pohlmeier**[a], **Pan Zhang**[b], **Xiaoying Hou**[b], **Heather A. Talbott**[b], **Robert A. Cushman**[c], **Jennifer R. Wood**[a], **John S. Davis**[b,d], **Andrea S. Cupp**[a,*]

[a]University of Nebraska–Lincoln, Animal Science, P.O. Box 830908, C203 ANSC, Lincoln, NE 68583-0908, USA2

[b]University of Nebraska Medical Center, Olson Center for Women's Health, 983255 Nebraska Medical Center, Omaha, NE 68198-3255, USA

[c]USDA, ARS, U.S. Meat Animal Research Center, Nutrition and Environmental Management Research, Spur 18D, Clay Center, NE 68933, USA

[d]VA Nebraska-Western Iowa Health Care System, Omaha, NE 68105, USA

Abstract

After ovulation, somatic cells of the ovarian follicle (theca and granulosa cells) become the small and large luteal cells of the corpus luteum. Aside from known cell type-specific receptors and steroidogenic enzymes, little is known about the differences in the gene expression profiles of these four cell types. Analysis of the RNA present in each bovine cell type using Affymetrix microarrays yielded new cell-specific genetic markers, functional insight into the behavior of each cell type via Gene Ontology Annotations and Ingenuity Pathway Analysis, and evidence of small and large luteal cell lineages using Principle Component Analysis. Enriched expression of select genes for each cell type was validated by qPCR. This expression analysis offers insight into cell-specific behaviors and the differentiation process that transforms somatic follicular cells into luteal cells.

Keywords

Bovine; Ovary; Follicle; Corpus luteum; Transcriptome; Cell identity

[*]Corresponding author. Acupp2@unl.edu (A.S. Cupp).

Author contribution statement

Dr. Romereim performed the data analysis and qPCR and wrote the manuscript with guidance and feedback from Drs. Wood, Davis, and Cupp. Dr. Adam Summers synchronized estrous cycles of cows to enable timed follicle collection. William Pohlmeier isolated the theca and granulosa cells with help from Drs. Wood and Cupp and performed the RNA isolation with Dr. Summers. Pan Zhang, Dr. Xiaoying Hou, and Heather A. Talbott performed the luteal cell collection, elutriation, and RNA isolation. Dr. Cushman provided manuscript feedback and analytical assistance via the Ingenuity® Pathway Analysis Software. Drs. Wood, Davis, and Cupp obtained the funding and determined the experimental design for this paper.

[1]Present address: New Mexico State University, Animal and Range Sciences, Knox Hall Room 202, MSC 3-1 Las Cruces, NM 88003, USA.

[2]ansc@unl.edu.

Declaration of interest

The authors have no conflicts of interest.

1. Introduction

1.1. Mammalian ovarian follicle and corpus luteum structure and function

A key feature of the mammalian female reproductive cycle is the ovarian follicle, which contains an oocyte, granulosa cells (GCs), and theca cells (TCs). The somatic GCs and TCs create a microenvironment that determines oocyte quality and maturation by synthesizing steroid and peptide hormones, secreting extracellular matrix, and signaling to control the development and health of the follicle/oocyte (Albertini et al., 2001; Hennet and Combelles, 2012). The TCs are primarily responsible for the synthesis of androgens within the ovary via the enzyme cytochrome P450 17A1 (CYP17A1) (Young and McNeilly, 2010). The mural GCs are positioned against the basement membrane on the periphery of the antrum while the cumulus GCs surround and can physically interact with the oocyte. Both of these GCs convert androgens to estrogens with the cytochrome P450 enzyme aromatase (CYP19A1) (Erickson and Hsueh, 1978). When ovulation occurs in response to a surge of luteinizing hormone (LH), the following series of events occurs: the follicle ruptures, the cumulus-oocyte-complex is released, and the remaining GCs and TCs differentiate into luteal cells as the ovulated follicle transforms into the corpus luteum (Stouffer and Hennebold, 2015). The morphology of the corpus luteum consists of large luteal cells (LLCs, ≥25 μm) and small luteal cells (SLCs, 12–25 μm) intermixed and accompanied by other cells that migrate into the tissue (Donaldson and Hansel, 1965; Fitz et al., 1982; Heath et al., 1983). Both LLCs and SLCs secrete progesterone, a steroid hormone that is required for the maintenance of pregnancy in most species including humans and cattle. However, in cows and sheep the SLCs contain the majority of the luteinizing hormone receptors (LHCGR) and the LLCs express the bulk of the prostaglandin F2 alpha (PGF2α) receptors (PTGFR) (Fitz et al., 1982; Mamluk et al., 1998; Wiltbank et al., 2012). The corpus luteum becomes highly vascularized in order to distribute progesterone, which inhibits the secretion of LH and thus prevents ovulation. For subsequent ovulation to occur the corpus luteum must regress, and this luteolysis can be triggered by PGF2α (Stouffer and Hennebold, 2015). Alternatively, when fertilization of the oocyte and implantation are successful, maternal recognition of pregnancy results in the maintenance of the corpus luteum which, in turn, plays a key role supporting the developing embryo. Anti-luteolytic mechanisms such as secretion of signaling molecules from the conceptus result in gene expression changes in the LLCs and SLCs (Romero et al., 2013). For example, both luteal cell types in ruminant species respond to the conceptus secretion of IFNT by increasing expression of ISG15 (interferon-stimulated gene, 15 kDa) (Romero et al., 2013). Thus, ovarian somatic cells play essential roles in oocyte and embryo fates.

1.2. Gene expression profiles of ovarian somatic cells

The physiological roles of GCs and TCs in the follicle are well studied in a variety of mammalian species including humans, non-human primates, rodents, sheep, and cattle (Edson et al., 2009). While there are some species-specific differences, many aspects of ovarian physiology are well conserved. A wide variety of microarray-based investigations have been performed in various species as well, often with the goal of understanding the changes in a single cell type in response to time, external stimuli, or disease conditions (Coskun et al., 2013; Kezele, 2005; McKenzie et al., 2004; Owens et al., 2002; Skinner et

al., 2008; Tsubota et al., 2011; Uyar et al., 2013; Wood et al., 2003; Xu et al., 2011). There are far fewer direct comparisons of the transcriptomes of specific cell types with the goal of identifying cell type markers and functional differences, but some have been performed including a recent direct comparison of the bovine GC and TC transcriptomes which identified cellular markers unique to GC and TC in addition to the traditional markers (steroidogenic enzymes and receptors) (Hatzirodos et al., 2015). Other studies have assessed the shifts in transcription patterns that occur in ovine and bovine GCs and TCs during follicular development (Bonnet et al., 2011 ; Hatzirodos et al., 2014a, b; Khan et al., 2016) or the gene expression changes in GCs and TCs during the attainment of follicle dominance and preovulatory status in the cow (Zielak et al., 2008) and the horse (Donadeu et al., 2014). However, characterization and comparison of the transcriptomes of GC and TC with LLC and SLC cell types is not currently available. Therefore, there is a gap in knowledge regarding how the follicular cells' gene expression profiles relate to the luteal phase of the reproductive cycle.

The transition from follicle to corpus luteum has also not been fully addressed by microarray analyses, though there are publications covering the short-term changes that happen in bovine GCs and TCs in response to the luteinizing hormone (LH) surge and intrafollicular prostanoids (Christenson et al., 2013; Li et al., 2009). A study of the GCs before and after human chorionic gonadotropin (hCG) administration in women undergoing controlled ovarian stimulation identified many of the same differentially expressed genes (Wissing et al., 2014). Other research conducted on the transcriptome of the corpus luteum has focused on the mechanisms of luteal regression in cattle and non-human primates (Bogan et al., 2009; Casey et al., 2005; Goravanahally et al., 2009) or on changes at progressive stages in the luteal life cycle (early, mid, mid-late, late, and very-late) (Bogan et al., 2008). However, these luteal microarrays did not distinguish between SLCs and LLCs.

1.3. Luteal cell type distinctions and lineages

There are currently no published microarray assessments of LLC and SLC gene expression profiles. What is known of the disparate functions of these cell types in sheep and cows comes from immunohistochemistiy, small-scale transcriptional analysis, and cell culture-based experiments. The major known functional differences are that the basal progesterone secretion of LLCs is about 6–20× greater than that of SLCs, but SLCs are able to robustly respond to LH to amplify their progesterone production while LLCs have a modest steroidogenic response to LH (Alila et al., 1988; Fitz et al., 1982; Harrison et al., 1987). Importantly, in addition to the lack of a comprehensive transcriptome for LLCs and SLCs, the question of their cellular origin and lineage has not been addressed with the latest technologies. The prevailing understanding is that in cows LLCs originate from the GCs that remain in the follicle after ovulation while the TCs give rise to SLCs (Donaldson and Hansel, 1965; Hansel et al., 1991). With new technology and a comprehensive assessment of the transcriptomes of the GC, TC, SLC, and LLC populations, possible lineage markers for future investigation can be identified in addition to attaining an improved understanding of the relative functions of each cell type. Thus the objective of this study was to comparatively analyze RNA microarrays of these four ovarian somatic cells in order to corroborate existing GC and TC transcriptomes, provide novel transcriptome data for LLCs and SLCs, perform

bioinformatic analyses to expand on the functional roles of these cells in ovarian physiology, and determine whether the existing luteal cell lineage model is supported by transcriptome analysis.

2. Methods

2.1. Follicular cell isolation

Follicular granulosa (n = 4 cows) and theca cells (n = 3 cows) were isolated from estrogen-active dominant follicles in ovaries of beef cows (75% Red Angus, 25% MARC III) from the physiology herd located at the University of Nebraska Agricultural Research and Development Center. The University of Nebraska-Lincoln Institutional Animal Care and Use Committee approved all procedures and facilities used in this experiment. Estrous cycles of cows were synchronized with a modified Co-Synch protocol using gonadotropin releasing hormone (GnRH) and a controlled internal drug release device (CIDR; 1.38 g progesterone, Zoetis) for 7 days with a PGF2α (25 mg/mL; Lutalyse, Pfizer Animal Health) injection at CIDR removal (Summers et al., 2014). Ovariectomy was performed approximately 36 h after CIDR removal (Youngquist et al., 1995). Upon ovariectomy, the largest (>10 mm diameter) antral follicle from each cow's ovaries was aspirated/dissected and the granulosa cells (≥94% purity), theca cells (≥82% purity), and follicular fluid were isolated as described previously (Summers et al., 2014). The purity of the follicular cell types using the same isolation method was determined by culturing 1 K cells per chamber on a 4-chamber glass slide, performing immunofluorescence detection of aromatase and smooth muscle actin, and manually counting the cells of six randomly selected regions. For the microarray, both granulosa and theca cells were homogenized in Tri-reagent (Sigma-Aldrich) for RNA isolation. It is important to note that follicles and RNA samples were collected from a large number of cows for use in various experiments, and those used for the microarray analyses were selected based on RNA quality and evidence of cell population enrichment. Thus, the GC and TC samples discussed in this article are not pairs from the same cows.

2.2. Luteal cell isolation

Luteal cells were isolated by elutriation from bovine corpora lutea of ovaries collected at a local abattoir (JBSSA, Omaha, NE) as described previously for cattle (Mao et al., 2013). Each corpus luteum (n = 3 cows for both LLC and SLC) was digested with collagenase to dissociate the cells, which were then suspended in a solution of DMEM (calcium free, 3.0 g/L glucose, 25 mM HEPES, 3.8 g/L sodium bicarbonate; 0.1% BSA, 0.02 mg/mL deoxyribonuclease, pH 7.2) to a total volume of 30 mL Elutriation was then performed with a Beckman Coulter Avanti-J20X centrifuge with a JE 5.0 rotor. The cells were applied to a Sanderson (Beckman) elutriation chamber and the eluates were collected with continuous flow with each fraction comprising 100 mL of eluate. Cell number, approximate size, and viability in collected fractions were determined with trypan blue staining using a hemocytometer. Most of the endothelial cell population was removed in the first fraction, as freshly isolated endothelial cells are smaller than SLCs (O'Shea et al., 1989). As described previously, the second and third collected fractions contained ≥90% SLCs, while the fourth fraction contained a majority of LLCs (≥80%) along with some SLC and endothelial cells

(Mao et al., 2013). Cells with a diameter of 15–25 μm were classified as small luteal cells, and cells with a diameter >30 μm were classified as large luteal cells. This approach provided direct confirmation of the composition of the cell populations, and the potential for a small proportion of cells to be retained that are of similar sizes to the luteal cells is considered in the analysis. The average purity of SLC in F2 and LLC in F4 were 93.6 ± 1.5% and 83.3 ± 0.9% (n = 3). SLCs and LLCs were concentrated with additional centrifugation of the relevant fractions, and the cells were homogenized in Tri-reagent (Sigma-Aldrich) for RNA isolation.

2.3. Microarray transcriptome analysis

After RNA extraction, 200 ng RNA for each sample were submitted to the University of Nebraska Microarray Core facility where the Affymetrix Bovine GeneChip® Gene 1.0 ST Array RNA expression analysis was performed. The microarray results were normalized with Robust Multi-Array Averaging. Array analysis was then performed using the National Institute of Aging tool (http://lgsun.grc.nia.nih.gov/ANOVA/) for Analysis of Variance (ANOVA), hierarchical clustering, and correlation between replicates. All functional bioinformatic analyses were performed on transcripts above a linear noise threshold of 100. Functional categorization of genes was determined by examining Gene Ontology Annotations (included in the Affymetrix microarray probe annotations) in combination with the gene descriptions from Entrez Gene (NCBI, http://www.ncbi.nlm.nih.gov/gene) and UniProtKB/Swiss-Prot (http://www.uniprot.org/). Predicted cell function outcomes were assessed with Ingenuity® Pathway Analysis (IPA; Winter 2015 release, Qiagen). The Principle Component Analysis was performed in R using script written in collaboration with the University of Nebraska-Lincoln Dept, of Statistics. Statistical significance of differences between Eigenvalues was determined with a two-tailed Student's T-tests with $P < 0.005$ indicating a significant difference.

2.4. Quantitative real-time PCR

To validate the microarray results, quantitative real-time PCR (qPCR) was performed in triplicate on 384-well plates to amplify select targets from cDNA synthesized from the RNA samples originally used for the microarray using the primers listed in Table 1. Power SYBR™ Green Master Mix (Thermo-Fisher) was utilized with an Applied Biosystems 7900HT Fast Real-Time PCR System. Expression was normalized to the geometric mean of the ribosomal RNA products RPL15 and RPL19. The results for each transcript are represented as fold-changes relative to the expression of that transcript in the cell type of interest.

3. Results and discussion

3.1. Cell type transcriptome clustering and correlation

To attain gene expression profiles for the somatic ovarian follicular and luteal cells, it was necessary to obtain a cell population that was highly enriched in a single cell type. Follicular cells were isolated from the ovaries of estrous-synchronized beef cows and the luteal cells were obtained from corpora lutea of beef cows from a local abattoir. The GC purity based on immunofluorescence (IF) against smooth muscle actin to detect any contaminating TCs was

≥94%. The TC population purity based on IF against aromatase to identify contaminating GCs was ≥82%. Using cell size, the LLC purity was ≥80% (contaminating cells may include clumps of endothelial cells or SLC and similarly sized fibroblasts or immune cells) and the SLC purity was ≥95% (contaminating cells may include clumps of endothelial cells or similarly sized fibroblasts or immune cells. Affymetrix RNA microarray analysis generated the transcriptome data (Romereim et al., 2016) [NCBI GEO GSE83524]. An overall low standard deviation profile indicated quality amplification, with slightly higher standard deviations for lower-intensity RNAs suggesting more variability for low copy-number targets [see Fig. 1 in accompanying Data in Brief article (Romereim et al., 2016)]. Hierarchical clustering to assess similarity between the gene expression profiles of the tissues showed that the follicular cell types (TC and GC) were similar to each other while the luteal cell types (LLC and SLC) were even more similar (Fig. 1A). The distance between branch points in the dendrogram, shown on the x-axis, indicates the degree of similarity between two samples (the shorter the distance, the greater the similarity in transcriptomes). The similar gene expression profiles of the luteal cells are likely due to their shared environment and related roles, but it is also important to note that the SLC and LLC samples are paired samples with each set originating from three different cows. In contrast, the GC and TC transcriptomes were not paired samples from the same cows but are still closely related on the dendrogram. The relationship between individual microarray replicates (each cell type from a separate cow) by hierarchical clustering confirmed that the gene expression profiles for all samples of the same cell type were highly similar (Fig. 1A). The degree of similarity in the samples' transcriptomes was also represented quantitatively by a correlation matrix that compares each microarray replicate against every other replicate (Fig. 1B). The correlation between each replicate of the same cell type was ≥97.5%, which indicates quality isolation methods and experimental reproducibility. Additional verification of experimental reproducibility is evident in sections 3.2.1 and 3.2.2, as specific GC and TC markers identified by other investigators were detected in the GC and TC microarrays (Christenson et al., 2013; Hatzirodos et al., 2015). The LLCs and SLCs were also highly similar to each other based on overall gene expression profile correlation, but as will be shown later these luteal cell types did have some interesting distinctions in gene expression. The TC overall expression profile was 92–95% correlated to the GCs, SLCs, and LLCs; while the GC expression profile was <90% similar to the SLCs and LLCs. This broad view of the similarities between the RNA expression of each cell type suggests similarities in function and cellular environment.

3.2. Differentially expressed genes for each cell type

The transcriptomes for the follicular and luteal cells were analyzed in two complementary ways. First, each individual microarray (linear intensity for all transcripts) was investigated using the Ingenuity Pathway Analysis (IPA) tools that predict the functional outcome of a given gene expression profile. Most of these results were highly similar for all four cell types due to the fact that they have the same housekeeping genes, basic cellular functions, and a shared ovarian environment. Some of the most prominent shared functions include cell death, cell survival, cell cycle progression, proliferation, RNA expression, protein metabolism, and organization of cytoplasm (Table 2). When the shared predicted functions are excluded, though, several interesting differences were apparent for each cell type.

The second analytical method used to assess the microarray data involved filtering the datasets so that only a subset of transcripts was used. Within each cell type there were sets of genes identified as differentially expressed for that cell type compared to the other three types [for a complete list see Tables 1, 2, 3, and 4 in (Romereim et al., 2016)]. Each set of genes that were differentially expressed (either ≥2-fold higher expression or ≥2-fold less compared to all three other cell types) was used for functional analyses (IPA, functional categorization) and to select targets for qPCR validation of the microarray results. The IPA input included the fold-changes for each transcript of the cell type of interest versus each of the other three cell types separately. Most of the differentially regulated genes were more highly expressed in their cell type, making them good candidates for cellular markers within the context of the ovarian follicle and corpus luteum. Six genes for each cell type were selected as marker genes (Table 3). Some published marker genes used to distinguish between GC and TC cells are also represented on this list. Preference for genes encoding membrane-bound proteins was also given to identify novel potential cell surface markers for flow cytometry and similar applications.

3.2.1. The GC transaiptome—The entire RNA expression profile of the GC samples revealed several features of the role of the GC in the ovary compared to the TCs, LLCs, and SLCs [available in (Romereim et al,, 2016)]. The shared housekeeping/ovarian predicted functions that were present in the other three cell types were predicted for the GC transcriptome, but there were also many GC-specific predicted functional outcomes (Table 4). Select predicted functions unique to the GCs indicate abundant expression of genes involved in S phase and G2 phase, more specifically than the general cell cycle progression predicted for the other cell types (Table 4). There was also gene expression associated with cellular colony formation (related to proliferation and cellular adhesion), RNA decay and repression, and protein complex assembly. Interestingly, several other predicted functions that are connected to G-protein coupled receptor or tyrosine kinase receptor signaling were specific to GCs such as the formation of clathrin-coated structures that internalize receptors, small GTPase-mediated signal transduction, and protein phosphorylation (Table 4). These functions are likely related to FSH signaling. The transcriptome of the dominant follicle GCs indicated a cell population with rapid proliferation, abundant G-protein coupled receptor signaling (e.g. FSH signaling), and modified RNA dynamics (RNA decay and repression).

Using the filtered set of genes that are differentially expressed in GCs, other distinguishing characteristics of the GC population can be determined to supplement those based on the global microarray results. The largest set of differentially expressed targets was identified for the GCs (452 enriched RNAs and 115 decreased compared to TCs, LLCs, and SLCs). Select genes including some well-known GC markers (*CYP19A1*, *FSHR*, and *INHBB*) were validated with qPCR (Fig. 2A). The entire set of genes enriched in GCs is available in the accompanying Data in Brief article [see Table 1 in (Romereim et al.(2016)]. Several of the genes enriched in the GC transcriptome were also identified as GC markers by Hatzirodos et al., in 2015, including *MGARP*, *GLDC*, *CHST8*, *SLC35G1*, *CA8*, *CLGN*, *FAM78A*, and *SLC16A3* [Table 1 in (Romereim et al., 2016; Hatzirodos et al., 2015)]. Only three of the markers in that article were not identified in the current microarray dataset: *LOC404103*,

CSN2, and *GPX3* (Hatzirodos et al., 2015). The minor differences in the GC markers identified likely lies in the methods and timing of cell collection. The GCs represented here are from the dominant follicle from a synchronized and tracked estrous cycle, while Hatzirodos et al., 2015, collected all follicles >9 mm from unsynchronized ovaries obtained from an abattoir (Hatzirodos et al., 2015). In Fig. 2B, the functional classifications of the GC-specific/enriched genes are shown. Increased RNA detection of genes involved in mitosis, DNA replication/repair/structure, and signal transduction was evident. These proliferation and signaling functions are known to be crucial for the role that GCs play in follicular maturation. Some signaling receptors included in the GC gene set were receptors for FSH, estrogen, Eph/ephrins, interleukin 6, insulin-like growth factor 1, and thrombin. There were also many effector molecules upregulated in GCs compared to the TC, LLC, and SLC gene set including SMADs, PLC, kinases involved in signaling cascades like MAPK3K5, and especially G-protein signaling modulators like Rac GTPases and GEFs. The IPA-predicted consequences of the genes differentially regulated in GCs is summarized in Table 4. The primary predictions included increases in cell proliferation, survival, DNA replication and repair, and microtubule/chromosome rearrangement. These predicted functions support the idea that proliferation is indeed central to the GC population. The overall results of these GC array analyses confirmed existing knowledge about GC markers and functions, provided a solid foundation for comparisons with the other ovarian somatic cells, and identified novel GC markers.

3.2.2. The TC transcriptome—The global RNA expression profile of the TCs included the same prominent, shared IPA predicted functions as the other three cell types (Table 2). The predicted functions unique to the TC transcriptome included many cellular behaviors related to metabolism including glycolysis, aerobic respiration, metabolism of heme, oxidation of protein, synthesis of carbohydrate, and synthesis of sterols (Table 5). Interestingly, insulin-like growth factor signaling and growth of ovarian follicles were also predicted specifically for the TC population and not for the other ovarian cell types (Table 5).

While the main conclusion of the predicted functions of the TC transcriptome was increased metabolic activities, the set of RNA transcripts enriched in TCs offered different insights. Of the set of genes differentially expressed in the TC samples compared to the GCs, LLCs, and SLCs [see Table 2 in (Romereim et al., 2016); 153 enriched RNAs and 11 decreased], selected targets were validated with qPCR (Fig. 3A). As with the GC gene expression profile, several of the genes enriched in these synchronized dominant follicle TC microarrays were also identified in unsynchronized ovaries by Hatzirodos et al., in 2015, as TC markers such as *DCN*, *COL1A2*, *COL3A1*, *OGN*, *COL5A2*, *NID1*, *ACTA2*, *ACTG2*, *EGFLAM*, *ADAMDEC1 HPGD*, *COL12A1*, *LOXL1*, and *RARRES1* [see Table 2 in (Romereim et al., 2016) (Hatzirodos et al., 2015)]. The TC gene set included a greater proportion of extracellular matrix genes than the other cell types as shown by Gene Ontology analysis (Fig. 3B). This included several collagens, elastin, decorin, fibrillin, and proteins that bind to or link extracellular matrix proteins. Other categories of genes enriched in TCs included signaling (such as receptors for PDGF, endothelin, and VIP as well as secreted molecules like INSL3 and SLIT2) and protein/nucleotide metabolism. The

traditional TC steroidogenic enzyme *CYP17A1* was also strongly enriched (Fig. 3A). Due to the smaller number of differentially expressed genes, the Ingenuity Pathway Analysis was only able to predict a small number of functions based on those genes, and few were relevant given the ovarian context (Table 5). For example, the predicted cell migration likely implies extracellular matrix remodeling and cytoskeletal dynamics rather than actual migration of theca cells. As with the GC array results, these TC transcriptomes analyses confirmed known marker genes and also indicated that the TC population is responsible for creating and modifying the extracellular matrix of the follicle, communicating with endothelial cells and GCs, and performing metabolic functions.

3.2.3. Shared genes enriched in both follicular cell types—The set of genes shared between the GC and TC populations that were enriched compared to both LLCs and SLCs provided information on what makes the follicular cells different from the luteal cells [see Table 5 in (Romereim et al., 2016); 708 enriched RNAs]. Functional analysis with IPA predicted that follicular cells (compared to luteal cells) have increased cell cycle progression and proliferation (multiple cyclins, cyclin-dependent kinases, and cell division cycle proteins), survival, organization of the cytoplasm and cytoskeleton (kinesins, dynein, cytoskeleton-associated proteins), and DNA replication and repair (e.g. *DNA2*, *FANCC*, *FANCI, RAD51*) (Table 6). This was accompanied by a predicted decrease in cell death, aneuploidy, and reproductive system hyperplasia. These predictions of active proliferation and growth are consistent with the known behavior of the dominant follicle just prior to the LH surge, the time when these samples were collected.

3.2.4. The LLC transcriptome—The IPA-predicted functional consequences of the entire set of LLC RNA transcripts included the typical housekeeping functions shared among all four cell types (Table 2) and also provided a variety of predicted functions specific to the LLCs. Many of these functions were related to adhesion (binding of cells, growth of epithelial tissue, and quantity of connective tissue) or cytoskeletal dynamics (microtubules and cell branching) (Table 7). These predicted cellular behaviors are consistent with the changes that occur during corpus luteum formation and LLC differentiation. Other functions included molecular transport, development of blood cells, production of reactive oxygen species, and cellular homeostasis (Table 7). The functions predicted for the LLC population did not include some known LLC behaviors such as lipid and protein production, but this is due to the fact that these are common to multiple cell types and were thus excluded by the analysis. The remaining LLC-specific functions covered behaviors necessary to maintain and support such a large cell including larger-scale cytoplasmic, membrane component, and cytoskeletal production/turnover.

In addition to the global cellular functions, the LLCs had a set of differentially expressed genes containing 300 enriched RNAs and 10 decreased transcripts when compared against the GC, TC, and SLC transcriptomes [see Table 3 in (Romereim et al., 2016)]. Selected genes were validated with qPCR, including the traditional LLC marker *PTGFR* (Fig. 4A). Of those genes specific to or enriched in the LLC samples, the greatest proportion was related to signaling (Fig. 4B). This includes receptors such as *PTGER3*, *PDGFR*, *PRLR*, *FLT1*, *KDR*, adrenergic receptor (*ADRA2B*), endothelin receptor (*EDNRB*), *TGFBR2*, and

TNFRSF21. As a note, prolactin regulates the luteotropic response in rodents but not in ruminants. Instead, prolactin is both produced within the bovine corpus luteum and regulates its vascularization (Erdmann et al., 2007; Shibaya et al., 2006). A specific role for prolactin signaling within in LLCs awaits discovery. Some secreted signaling molecules represented were *VEGFA*, *PDGFA*, *PTHLH*, and *KHIG*. The IPA predicted functional outcome of the LLC enriched set of genes included angiogenesis/vasculogenesis (.*EFNB2*, *PDGFRB*, VECFA), differentiation of cells (*NOTCH3*, *PTHLH, TGFBR2, WNT11*), immune and inflammatory response (chemo-kines, interleukins, tumor necrosis factor family molecules), synthesis of lipid (*AC0X2*, ACSL4, *CYP7B1*, *RDH10*), and ion transport (*SLC7A8*, *ATP1B2*) (Table 7). Overall, these data showed that the LLC population is actively engaged in cell-cell communication to recruit immune/endothelial cells as well as synthesize lipids while maintaining the adhesion, cytoskeleton, and homeostasis needed to support its large size.

3.2.5. The SLC transaiptome—The global SLC microarray results had many predicted functional consequences based on IPA, including those common to all four cell types (Table 2). Among the predicted functions that were exclusive to the SLCs, many specific types of metabolism were found including metabolism of phospholipids, peptides, and sterols as well as regulation of the concentration of ATP (Table 8). Other functions were related to signal transduction such as dephosphorylation of proteins and oxidative stress response (Table 8). And, interestingly, cellular storage in the form of inclusion bodies made a sole appearance on the SLC list in addition to the transport of molecules and fluid into cells by pinocytosis (Table 8). The large-scale transcript comparison thus suggested that the SLCs were performing different metabolic, signaling, and storage functions than LLCs and follicular cells.

While the whole SLC transcriptome yielded a wide variety of results, the SLC samples had the fewest differentially represented RNAs with 48 increased and 12 decreased relative to GCs, TCs, and LLCs [see Table 4 in (Romereim et al., 2016)]. A few select genes were validated by qPCR (Fig. 5A) including the canonical SLC marker *LHCGR*. It has been previously determined that the SLCs contain the majority of LH receptors in the bovine corpus luteum, but that *LHCGR* expression does occur in the bovine LLCs (Mamluk et al., 1998). However, the *LHCGR* expression activity in the LLCs can change based on external stimuli such as seasonal changes and exogenous hormonal treatments, suggesting the possibility that the disparity in SLC and LLC *LHCGR* expression may vary (Wiltbank, 1994). Additionally, *LHCGR* is even less suited to be a marker gene when all four cell types are considered since that gene is expressed in both GCs and TCs (with the level of expression depending on the stage in follicular development). The greatest number of the genes were involved in signal transduction (Fig. 5B). This included both receptors and ligands related to BMP signaling, complement components involved in immune response, and effector molecules such as kinases and phospholipases. Interestingly, the receptor *KIT* was present in the SLCs that corresponds to the *KITLG* produced by the LLCs. Previous work has also demonstrated that TCs express *KIT* to communicate with GCs, which express *KITLG* (Parrott and Skinner, 1997). Due to the small set of genes involved, functional assessment with IPA yielded only two predicted increased behaviors: aggregation of

platelets and cancer (Table 8). Neither prediction shed much extra light on the SLCs within the context of ovarian biology. The set of genes enriched in SLCs, however, was useful in determining the distinguishing characteristics between LLCs and SLCs, which were primarily the predominant active signaling pathways and some differences in extracellular matrix (*COL6A1*, *MMP7*, *CCBE1*) and adhesion (*CLDN1*).

3.2.6. Shared genes enriched in both luteal cell types—When comparing the luteal cells as a group to the follicular cells, 792 RNA transcripts were enriched in the LLC and SLC populations together compared to both the GC and TC samples [see Table 6 in (Romereim et al., 2016)]. IPA assessment of the transcripts enriched in both luteal cell types indicated increased metabolism/synthesis of lipids and steroids (cholesterol, eicosanoid, sterol, terpenoid, fatty acids, lipid membranes), cellular proliferation and survival, cell maturation, increased quantity of gonad, inflammatory and immune response, angiogenesis and migration of endothelial cells, and cell-to-cell signaling among other functions (Table 9). An additional consideration with the luteal cell microarrays is that the process of elutriation causes mechanical stresses to the cells. The duration of the elutriation may allow transcription of some early-response stress genes. Shared luteal cell microarray detection of RNAs such as *JUN*, *JUNB*, *JUND*, *NFKB2*, *EGR1*, *EGR2*, FOS, and *FOSB* could be due to in vivo signaling responses or to the cellular isolation procedure.

3.3. Gene expression patterns and Principle Component Analysis

Beyond determining differentially expressed gene sets and evaluating the predicted functional consequences, another method to analyze large datasets is Principle Component Analysis (PCA). With this statistical tool, patterns of gene expression are grouped into Principle Components (PC) that have their own Eigenvector (a vector within a matrix) and each sample is given an Eigenvalue corresponding to how well it fits each PC (i.e. gene expression pattern). The first PC explains the most variation within the dataset, and two to three PCs should incorporate almost all of the variation. If two or three PCs are graphed (either in two dimensions or in 3D) with the Eigenvalues converted to graphing coordinates, the variation between samples is easily visualized. A two-dimensional representation of PC1 and PC2 shows that the microarray replicates of the same cell type clustered together (Fig. 6). This supported the hierarchical clustering results shown in Fig. 1A. However, unlike with hierarchical clustering based on the global transcriptome for each microarray replicate, PCA emphasizes variability in the data to tease out potential relationships and make those relationships easier to visualize. In Fig. 6, using PC1 (which covers 79.15% of the expression variance) as the x-axis placed the LLC and SLC populations adjacent to each other (and not statistically significant via *t*-test) and indicated their close relationship in terms of gene expression patterns. Interestingly, the GC and TC populations were furthest apart (emphasizing variability between the two populations) but TC and SLC were next to each other and the LLC and GC samples were also adjacent (and had mean PC1 eigenvalues that are not significantly different). This suggested a relationship between GC and LLC and between TC and SLC, supporting the existing lineage model. However, PCA cannot conclusively establish lineages, so future studies are needed to directly demonstrate this model.

3.4. Transcriptional effects of GC and TC luteinization

Based on these microarrays, there were markers that are highly enriched or specific to each cell type and also potential lineage markers based on genes that were enriched in both GCs and LLCs or in both TCs and SLCs (Table 2, Fig. 7). The process of luteinization is a dramatic change in the morphology and function of the follicle, so the substantial differences in the gene expression profiles of the follicular cells and the luteal cells is understandable. Previous microarray analyses have investigated the TCs and GCs immediately before and after the LH surge that triggers ovulation and luteinization. Thus, it is possible to look for gene expression changes in the TCs and GCs caused by the LH surge that could be maintained by SLCs and LLCs. Based on microarray data from Christenson et al., 2013, some specific gene expression changes in GCs and TCs in response to the LH surge are compatible with a transition to specific luteal cell types.

While the synchronized dominant follicles for these GC and TC microarrays were collected approximately 36 h after injection with PGF2α to harvest pre-ovulatory follicular cells, the dominant follicles for the Christenson et al., 2013, microarrays were either collected without PGF2α during the height of the first follicular wave (pre-LH samples) or after a series of injections to create an LH surge (PGF2α, a 48-h wait, a GnRH analog injection, and another 23-h wait to allow the cells time to respond to the LH) (Christenson et al., 2013). The GCs and TCs compared here to luteal cells and the periovulatory/post-LH GCs and TCs from Christenson et al., 2013, are thus only separated by approximately 36 h (with the data in this manuscript providing the earlier time point) and an LH surge. The transformation that happens during that event, however, provides an intermediate step between follicular cells and luteal cells. As part of that shift, there were gene expression changes in TCs in response to the LH surge that are compatible with a transition to an SLC phenotype including a decrease in expression of *CYP17A1, SLC1A3, TRAF5, TSPAN33*, and *HPGD* concurrent with increased expression of *RHOB* [see Table 4 in (Romereim et al., 2016)] (Christenson et al., 2013). There were even more parallels when assessing the effects of the LH surge on GCs. The loss of GC expression of *CYP19A1*, *CHST8, HSD17B1, GCLC, SLC35G1*, and *GPT* along with the gain of expression of *PTX3, RUNX2, POSTN*, *RND3, TIMP1, NTS, FOS*, and *RCAN1* are all consistent with a switch from a GC transcriptome to an LLC gene expression profile [see Table 3 in (Romereim et al., 2016)] (Christenson et al., 2013). Thus, comparing microarray results provides an idea of the immediate changes during luteinization that are maintained when the luteal phenotype is attained.

4. Conclusions

After analyzing the RNA profiles of the follicular GCs and TCs and the LLCs and SLCs of the corpus luteum, we have determined cellular expression markers for each population (both novel genes and validation of previously identified markers). We have also assessed the functional implications of the differentially expressed genes for each cell type and follicular/luteal cells as groups. These analyses are especially beneficial for the LLCs and the SLCs, for which no transcriptome analysis is yet published. Further microarray comparative analysis has provided both support and potential markers for the lineage model that predicts that LLCs come from GCs and TCs primarily differentiate into SLCs.

Acknowledgements

The authors would like to acknowledge the assistance of the University of Nebraska Medical Center Microarray Core Facility for performing the microarrays and the University of Nebraska-Lincoln Department of Statistics for their help in incorporating the Principle Component Analysis. The University of Nebraska Microarray Core receives partial support from the National Institute for General Medical Science (NIGMS) INBRE - P20GM103427–14 and COBRE −1P30GM110768–01 grants as well as The Fred & Pamela Buffett Cancer Center Support Grant - P30CA036727. This publication's contents are the sole responsibility of the authors and do not necessarily represent the official views of the NIH or NIGMS.

Support

This research was supported by USDA Hatch grant NEB26–202/W2112 to ASC, Hatch -NEB ANHL 26–213 to ASC and JRW, NEB 26–206 to ASC and JRW, NIFA 2013–67015-20965 to ASC, JRW and JSD, NIFA grant 2011–67015-20076 to JSD and ASC, postdoctoral fellowship 2016–67012-24697 to SMR, and predoctoral fellowship 2014–67011-22280 to HAT. USDA is an equal opportunity provider and employer. Names are necessary to report factually on available data; however, the USDA neither guarantees nor warrants the standard of the product, and the use of names by the USDA implies no approval of the product to the exclusion of others that may also be suitable. The research was also supported by funds from the VA Research and Development service.

Abbreviations:

GC	granulosa cell
IPA	Ingenuity® Pathway Analysis
LLC	large luteal cell
PC	principle component
PCA	principle component analysis
SLC	small luteal cell; TC, theca cell

References

Albertini DF, Combelles CMH, Benecchi E, Carabatsos MJ, 2001 Cellular basis for paracrine regulation of ovarian follicle development. Reproduction 121, 647–653. http://dx.doi.Org/10.1530/reprod/121.5.647. [PubMed: 11427152]

Alila HW, Dowd JP, Corradino R. a, Harris WV, Hansel W., 1988 Control of progesterone production in small and large bovine luteal cells separated by flow cytometry. Reproduction 82, 645–655. 10.1530/jrf.0.0820645.

Bogan RL, Murphy MJ, Hennebold JD, 2009 Dynamic changes in gene expression that occur during the period of spontaneous functional regression in the rhesus macaque corpus luteum. Endocrinology 150, 1521–1529. 10.1210/en.2008-1201. [PubMed: 18948396]

Bogan RL, Murphy MJ, Stouffer RL, Hennebold JD, 2008 Systematic determination of differential gene expression in the primate corpus luteum during the luteal phase of the menstrual cycle. Mol. Endocrinol 22, 1260–1273. 10.1210/me.2007-0484. [PubMed: 18258683]

Bonnet A, Bevilacqua C, Benne F, Bodin L, Cotinot C, Liaubet L, Sancristobal M, Sarry J, Terenina E, Martin P, Tosser-Klopp G, Mandon-Pepin B, 2011 Transcriptome profiling of sheep granulosa cells and oocytes during early follicular development obtained by Laser Capture Microdissection. BMC Genomics 12, 417 10.1186/1471-2164-12-417. [PubMed: 21851638]

Casey OM, Morris DG, Powell R, Sreenan JM, Fitzpatrick R, 2005 Analysis of gene expression in non-regressed and regressed bovine corpus luteum tissue using a customized ovarian cDNA array. Theriogenology 64,1963–1976. 10.1016/j.theriogenology.2005.04.015. [PubMed: 15953631]

Christenson LK, Gunewardena S, Hong X, Spitschak M, Baufeld A, Vanselow J, 2013 Research resource: preovulatory LH surge effects on follicular theca and granulosa transcriptomes. Mol. Endocrinol 27, 1153–1171. 10.1210/me.2013-lQ93. [PubMed: 23716604]

Coskun S, Otu HH, Awartani KA., Al-Alwan LA, Al-Hassan S, Al-Mayman H, Kaya N, Inan MS, 2013 Gene expression profiling of granulosa cells from PCOS patients following varying doses of human chorionic gonadotropin. J. Assist. Reprod. Genet 30, 341–352. 10.1007/sl0815-Q13-9935-y. [PubMed: 23381551]

Donadeu FX, Fahiminiya S, Esteves CL, Nadaf J, Miedzinska K, McNeilly AS, Waddington D, Gérard N, 2014 Transcriptome profiling of granulosa and theca cells during dominant follicle development in the horse. Biol. Reprod 91, 111 10.1095/biolreprod.l14.118943. [PubMed: 25253738]

Donaldson L, Hansel W, 1965 Histological study of bovine corpora lutea. J. Dairy Sci 48, 905–909. 10.3168/jds.S0022-0302(65)88360-6. [PubMed: 14330748]

Edson MA, Nagaraja AK, Matzuk MM, 2009 The mammalian ovary from genesis to revelation. Endocr. Rev. 30, 624–712. 10.1210/er.2009-0012. [PubMed: 19776209]

Erdmann S, Ricken A, Merkwitz C, Struman L, Castino R, Hummitzsch K, Gaunitz F, Isidora C, Martial J, Spanel-Borowski K, 2007 The expression of prolactin and its cathepsin D-mediated cleavage in the bovine corpus luteum vary with the estrous cycle. Am. J. Physiol. Endocrinol. Metab 293, E1365–E1377. 10.1152/ajpendo.00280.2007. [PubMed: 17785503]

Erickson GF, Hsueh AJ, 1978 Stimulation of aromatase activity by follicle stimulating hormone in rat granulosa cells in vivo and in vitro. Endocrinology 102, 1275–1282. 10.1210/endo-102-4-1275. [PubMed: 744025]

Fitz TA., Mayan MH, Sawer HR, Niswender GD, 1982 Characterization of two steroidogenic cell types in the ovine corpus luteum. Biol. Reprod 27, 703–711. http://dx.doi.Org/10.1095/biolreprod27.3.703. [PubMed: 6291651]

Goravanahally MP, Salem M, Yao J, Inskeep EK, Flores J.a., 2009 Differential gene expression in the bovine corpus luteum during transition from early phase to midphase and its potential role in acquisition of luteolytic sensitivity to prostaglandin F2 alpha. Biol. Reprod 80, 980–988. 10.1095/biolreprod.108.069518. [PubMed: 19164179]

Hansel W, Alila HW, Dowd j.P., Milvae RA, 1991 Differential origin and control mechanisms in small and large bovine luteal cells. J. Reprod. Fertil Suppl. 43, 77–89.

Harrison LM, Kenny N, Niswender GD, 1987 Progesterone production, LH receptors, and oxytocin secretion by ovine luteal cell types on days 6, 10 and 15 of the oestrus cycle and day 25 of pregnancy. J. Reprod. Fertil 79, 539–548. 10.1530/jrf.0.0790539. [PubMed: 3572885]

Hatzirodos N, Hummitzsch K, Irving-Rodgers HF, Rodgers RJ, 2015 Transcriptome comparisons identify new cell markers for theca interna and granulosa cells from small and large antral ovarian follicles. PLoS One 10, 1–13. 10.1371/joumal.pone.0119800.

Hatzirodos N, Hummitzsch IC, Irving-Rodgers HF, Rodgers RJ, 2014a Transcriptome profiling of the theca interna in transition from small to large antral ovarian Follicles. PLoS One 9 10.1371/joumal.pone.0097489.

Hatzirodos N, Irving-Rodgers HF, Hummitzsch K, Harland ML, Morris SE, Rodgers RJ, 2014b Transcriptome profiling of granulosa cells of bovine ovarian follicles during growth from small to large antral sizes. BMC Genomics 15, 24 10.1186/1471-2164-15-24. [PubMed: 24422759]

Heath E, Weinstein P, Merritt B, Shanks R, Hixon J, 1983 Effects of prostaglandins on the bovine corpus luteum: granules, lipid inclusions and progesterone secretion. Biol. Reprod 29, 977–985. 10.1095/biolreprod29.4.977. [PubMed: 6315098]

Hennet ML, Combelles CMH, 2012 The antral follicle: a microenvironment for oocyte differentiation. Int. J. Dev. Biol 56, 819–831. 10.1387/ijdb.l20133cc [PubMed: 23417404]

Kezele PR, 2005 Alterations in the ovarian transcriptome during primordial follicle assembly and development. Biol. Reprod 72, 241–255. 10.1095/biolreprod.l04.032060. [PubMed: 15371273]

Khan DR, Fournier E, Dufort I, Richard FJ, Singh J, Sirard MA, 2016 Metaanalysis of gene expression profiles in granulosa cells during folliculogenesis. Reproduction 15 10.1530/REP-15-0594.

Li Q, Jimenez-Krassel F, Ireland JJ, Smith GW, 2009 Gene expression profiling of bovine preovulatory follicles: gonadotropin surge and prostanoid-dependent up-regulation of genes potentially linked to the ovulatory process. Reproduction 137, 297–307. 10.1530/REP-08-0308. [PubMed: 18996975]

Mamluk R, Chen D, Greber Y, Davis JS, Meidan R, 1998 Characterization of messenger ribonucleic acid expression for prostaglandin F2 alpha and luteinizing hormone receptors in various bovine luteal cell types. Biol. Reprod 58, 849–856. http://dx.doi.Org/10.1095/biolreprod58.3.849. [PubMed: 9510976]

Mao D, Hou X, Talbott H, Cushman R, Cupp A, Davis JS, 2013 ATF3 expression in the corpus luteum: possible role in luteal regression. Mol. Endocrinol 27, 2066–2079. http://dx.doi.Org/10.l210/me.2013-1274. [PubMed: 24196350]

McKenzie LJ, Pangas SA, Carson SA, Kovanci E, Cisneros P, Buster JE, Amato P, Matzuk MM, 2004 Human cumulus granulosa cell gene expression: a predictor of fertilization and embryo selection in women undergoing IVF. Hum. Reprod 19, 2869–2874. 10.1093/humrep/deh535. [PubMed: 15471935]

O'Shea JD, Rodgers RJ, D'Occhio MJ, 1989 Cellular composition of the cyclic corpus luteum of the cow. J. Reprod. Fertil 85, 483–487. 10.1530/jrf.0.0850483. [PubMed: 2703988]

Owens GE, Keri RA, Nilson JH, 2002 Ovulatory surges of human CG prevent hormone-induced granulosa cell tumor formation leading to the identification of tumor-associated changes in the transcriptome. Mol. Endocrinol 16, 1230–1242. http://dx.doi.Org/10.1210/me.16.6.1230. [PubMed: 12040011]

Parrott JA, Skinner MK, 1997 Direct actions of kit-ligand on theca cell growth and differentiation during follicle development. Endocrinology 138, 3819–3827. http://dx.doi.Org/10.1210/en.138.9.3819. [PubMed: 9275070]

Romereim SM, Summers AF, Pohlmeier WE, Hou X, Talbott HA, Cushman RA, Wood JR, Davis JS, Cupp AS, 2016 Transcriptomes of Bovine Ovarian Follicular and Luteal Cells. Data Br. in press.

Romero JJ, Antoniazzi AQ, Smirnova NP, Webb BT, Yu F, Davis JS, Hansen TR, 2013 Pregnancy-associated genes contribute to antiluteolytic mechanisms in ovine corpus luteum. Physiol. Genomics 45,1095–1108. 10.1152/physiolgenomics.00082.2013. [PubMed: 24046284]

Shibaya M, Murakami S, Tatsukawa Y, Skarzynski DJ, Acosta TJ, Okuda K, 2006 Bovine corpus luteum is an extrapituitary site of prolactin production. Mol. Reprod. Dev 73, 512–519. 10.1002/mrd.20445. [PubMed: 16435374]

Skinner MK, Schmidt M, Savenkova MI, Sadler-Riggleman I, Nilsson EE, 2008 Regulation of granulosa and theca cell transcriptomes during ovarian antral follicle development. Mol. Reprod. Dev 75, 1457–1472. 10.1002/mrd.20883. [PubMed: 18288646]

Stouffer RL, Hennebold JD, 2015 Structure, function, and regulation of the corpus luteum. In: Knobil and Neill's Physiology of Reproduction, fourth ed. Elsevier Inc 10.1016/B978-0-12-397175-3.00023-5.

Summers AF, Pohlmeier WE, Sargent KM, Cole BD, Vinton RJ, Kurz SG, McFee RM, Cushman R. a, Cupp AS, Wood JR, 2014 Altered theca and cumulus oocyte complex gene expression, follicular arrest and reduced fertility in cows with dominant follicle follicular fluid androgen excess. PLoS One 9, e110683 10.1371/journal.pone.O110683. [PubMed: 25330369]

Tsubota K, Kanki M, Noto T, Shiraki K, Takeuchi A, Nakatsuji S, Seki J, Oishi Y, Matsumoto M, Nakayama H, 2011 Transitional gene expression profiling in ovarian follicle during ovulation in normal-cycle rats. Toxicol. Pathol 39, 641–652. 10.1177/0192623311406932. [PubMed: 21551027]

Uyar A, Torrealday S, Seli E, 2013 Cumulus and granulosa cell markers of oocyte and embryo quality. Fertil. Steril 99, 979–997. 10.1016/j.fertnstert.2013.01.129. [PubMed: 23498999]

Wiltbank MC, 1994 Cell types and hormonal mechanisms associated with midcycle corpus luteum function. J. Anim. Sci 72,1873–1883. [PubMed: 7928767]

Wiltbank MC, Salih SM, Atli MO, Luo W, Bormann CL, Ottobre JS, Vezina CM, Mehta V, Diaz FJ, Tsai SJ, Sartori R, 2012 Comparison of endocrine and cellular mechanisms regulating the corpus luteum of primates and ruminants. Anim. Reprod 9, 242–259. 10.1016/j.biotechadv.2011.08.021.Secreted. [PubMed: 23750179]

Wissing ML, Kristensen SG, Andersen CY, Mikkelsen AL, Host T, Borup R, Grondahl ML, 2014 Identification of new ovulation-related genes in humans by comparing the transcriptome of granulosa cells before and after ovulation triggering in the same controlled ovarian stimulation cycle. Hum. Reprod 29, 997–1010. 10.1093/humrep/deu008. [PubMed: 24510971]

Wood JR, Nelson VL, Ho C, Jansen E, Wang CY, Urbanek M, McAllister JM, Mosselman S, Strauss JF, 2003 The molecular phenotype of polycystic ovary syndrome (PCOS) theca cells and new candidate PCOS genes defined by microarray analysis. J. Biol. Chem 278, 26380–26390. 10.1074/jbc.M300688200. [PubMed: 12734205]

Xu F, Stouffer RL, Müller J, Hennebold JD, Wright JW, Bahar A, Leder G, Peters M, Thorne M, Sims M, Wintermantel T, Lindenthal B, 2011 Dynamics of the transcriptome in the primate ovulatory follicle. Mol. Hum. Reprod 17,152–165. 10.1093/molehr/gaq089. [PubMed: 21036944]

Young JM, McNeilly a S., 2010 Theca: the forgotten cell of the ovarian follicle. Reproduction 140, 489–504. 10.1530/REP-10-0094. [PubMed: 20628033]

Youngquist RS, Garverick HA, Keisler DH, 1995 Use of umbilical cord clamps for ovariectomy in cows. J. Am. Vet. Med. Assoc 207, 474–475. [PubMed: 7591949]

Zielak AE, Canty MJ, Forde N, Coussens PM, Smith GW, Lonergan P, Ireland JJ, Evans ACO, 2008 Differential expression of genes for transcription factors in theca and granulosa cells following selection of a dominant follicle in cattle. Mol. Reprod. Dev 75, 904–914. 10.1002/mrd.20819. [PubMed: 17948250]

A. Hierarchical Clustering of Microarray Replicates

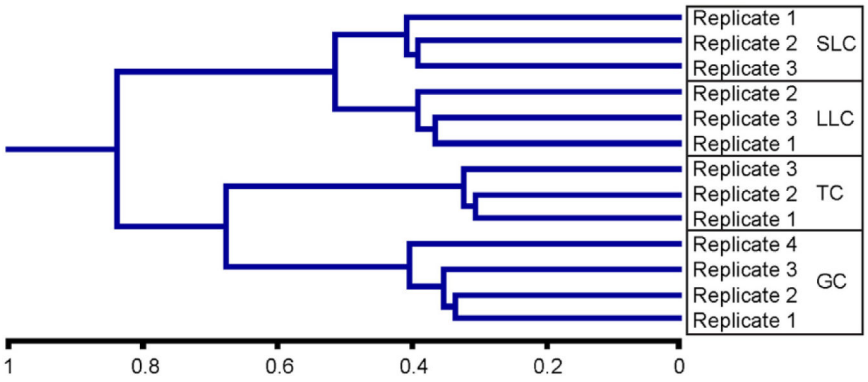

B. Correlation Matrix of Microarray Replicates

	GC Rep 1	GC Rep 2	GC Rep 3	GC Rep 4	TC Rep 1	TC Rep 2	TC Rep 3	LLC Rep 1	LLC Rep 2	LLC Rep 3	SLC Rep 1	SLC Rep 2	SLC Rep 3
GC Rep 1	1	0.984	0.982	0.975	0.946	0.935	0.940	0.877	0.879	0.877	0.891	0.889	0.891
GC Rep 2	0.984	1	0.983	0.981	0.940	0.928	0.933	0.868	0.871	0.869	0.883	0.883	0.886
GC Rep 3	0.982	0.983	1	0.977	0.949	0.938	0.943	0.880	0.884	0.881	0.893	0.894	0.896
GC Rep 4	0.975	0.981	0.977	1	0.935	0.925	0.930	0.862	0.864	0.864	0.876	0.877	0.879
TC Rep 1	0.946	0.940	0.949	0.935	1	0.987	0.985	0.923	0.926	0.923	0.932	0.934	0.931
TC Rep 2	0.935	0.928	0.938	0.925	0.987	1	0.987	0.926	0.930	0.926	0.932	0.936	0.931
TC Rep 3	0.940	0.933	0.943	0.930	0.985	0.987	1	0.925	0.929	0.928	0.932	0.934	0.932
LLC Rep 1	0.877	0.868	0.880	0.862	0.923	0.926	0.925	1	0.978	0.981	0.965	0.958	0.957
LLC Rep 2	0.879	0.871	0.884	0.864	0.926	0.930	0.929	0.978	1	0.980	0.968	0.966	0.966
LLC Rep 3	0.877	0.869	0.881	0.864	0.923	0.926	0.928	0.981	0.980	1	0.962	0.958	0.961
SLC Rep 1	0.891	0.883	0.893	0.876	0.932	0.932	0.932	0.965	0.968	0.962	1	0.976	0.976
SLC Rep 2	0.889	0.883	0.894	0.877	0.934	0.936	0.934	0.958	0.966	0.958	0.976	1	0.978
SLC Rep 3	0.891	0.886	0.896	0.879	0.931	0.931	0.932	0.957	0.966	0.961	0.976	0.978	1

Fig. 1.

Hierarchical clustering and correlation matrix of all microarray replicates. (A) Hierarchical cluster dendrograms indicate the degree of similarity between cell types and individual replicates using the distance at which the branch point occurs. The replicates within a cell type cluster closely together, and the two follicular cell types and two luteal cell types also cluster together. (B) The correlation matrix allows a quantitative comparison of any two microarray replicates. A correlation value of 1 indicates that the two replicates compared are identical, and the correlation between each replicate of the same cell type is ≥ 97.5% (red). The large luteal cells (LLCs) and small luteal cells (SLCs) are also highly similar (>95% and <97%, red), the theca cells (TCs) have an overall expression profile that is 92–95% correlated to the granulosa cells (GCs), SLCs, and LLCs (orange), and the GC expression profile is <90% similar to the SLCs and LLCs (yellow). (For interpretation of the references to colour in this figure legend, the reader is referred to the web version of this article.)

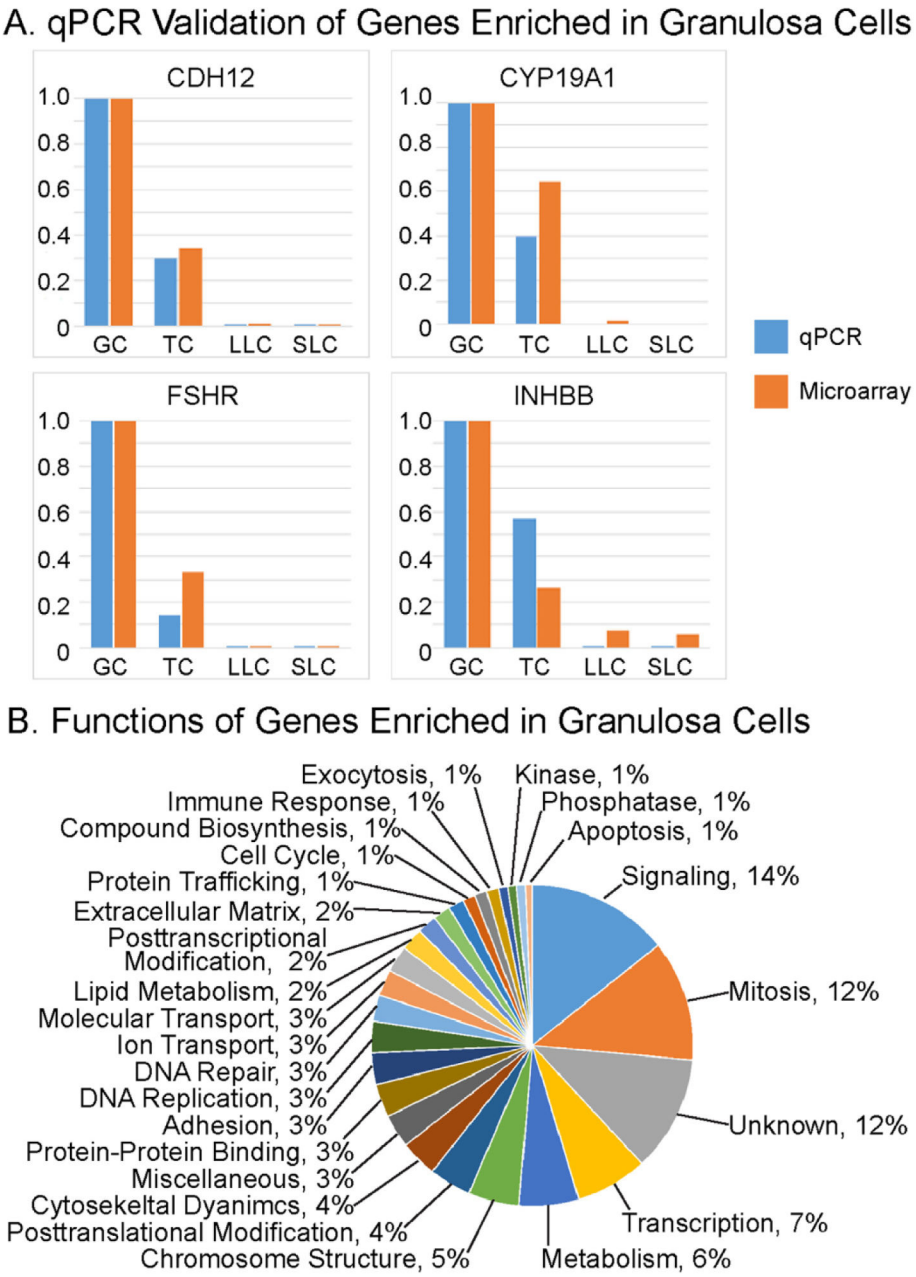

Fig. 2.

Granulosa cell-enriched gene set validation and functional categorization. (A) Validation of select granulosa cell (GC)-enriched genes with qPCR (blue) compared to the microarray fold changes (orange). (B) Functional categorization of genes enriched in GC samples shown as a percentage of the 567 differentially regulated transcripts.

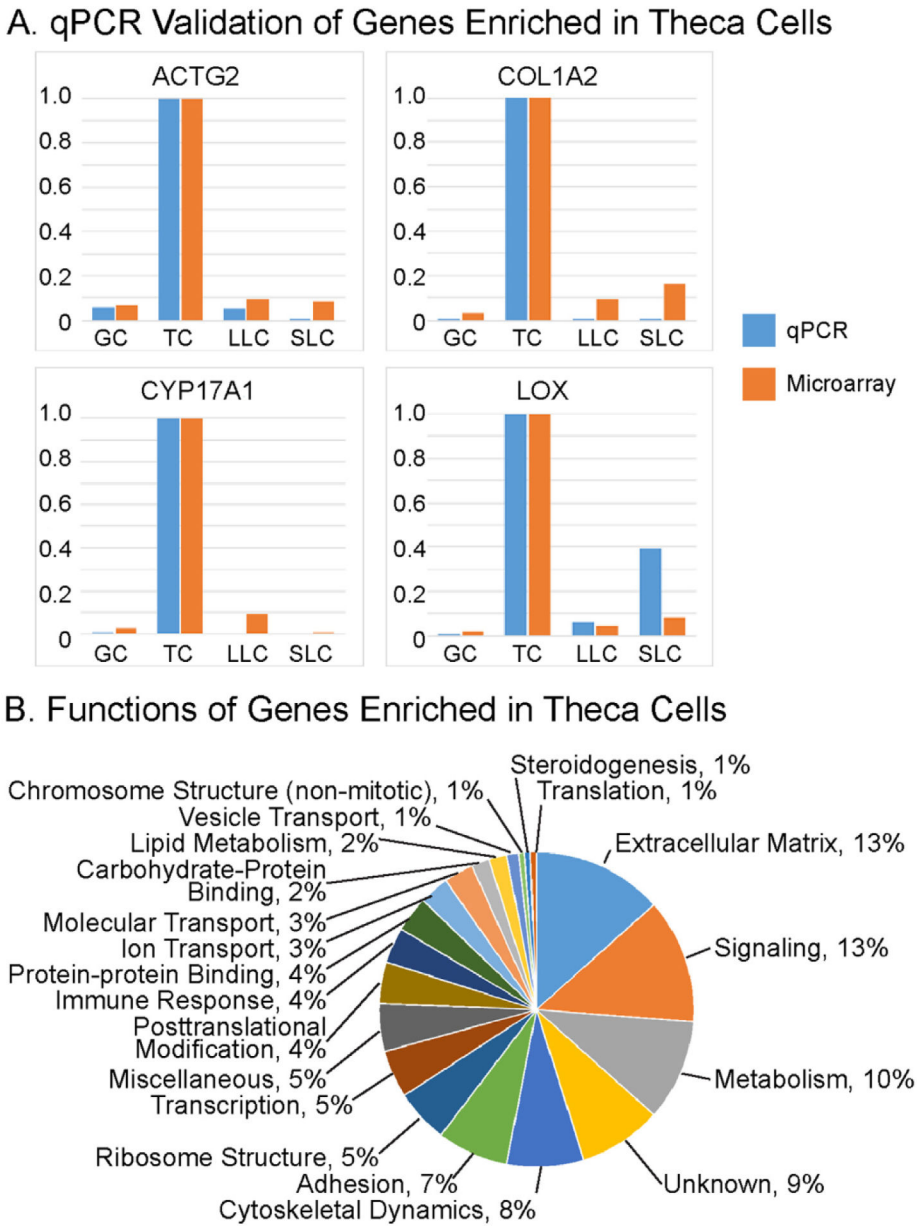

Fig. 3.

Theca cell-enriched gene set validation and functional categorization. (A) Validation of select theca cell (TC)-enriched genes with qPCR (blue) compared to the microarray fold changes (orange). (B) Functional categorization of genes enriched in TC samples shown as a percentage of the 164 differentially regulated transcripts.

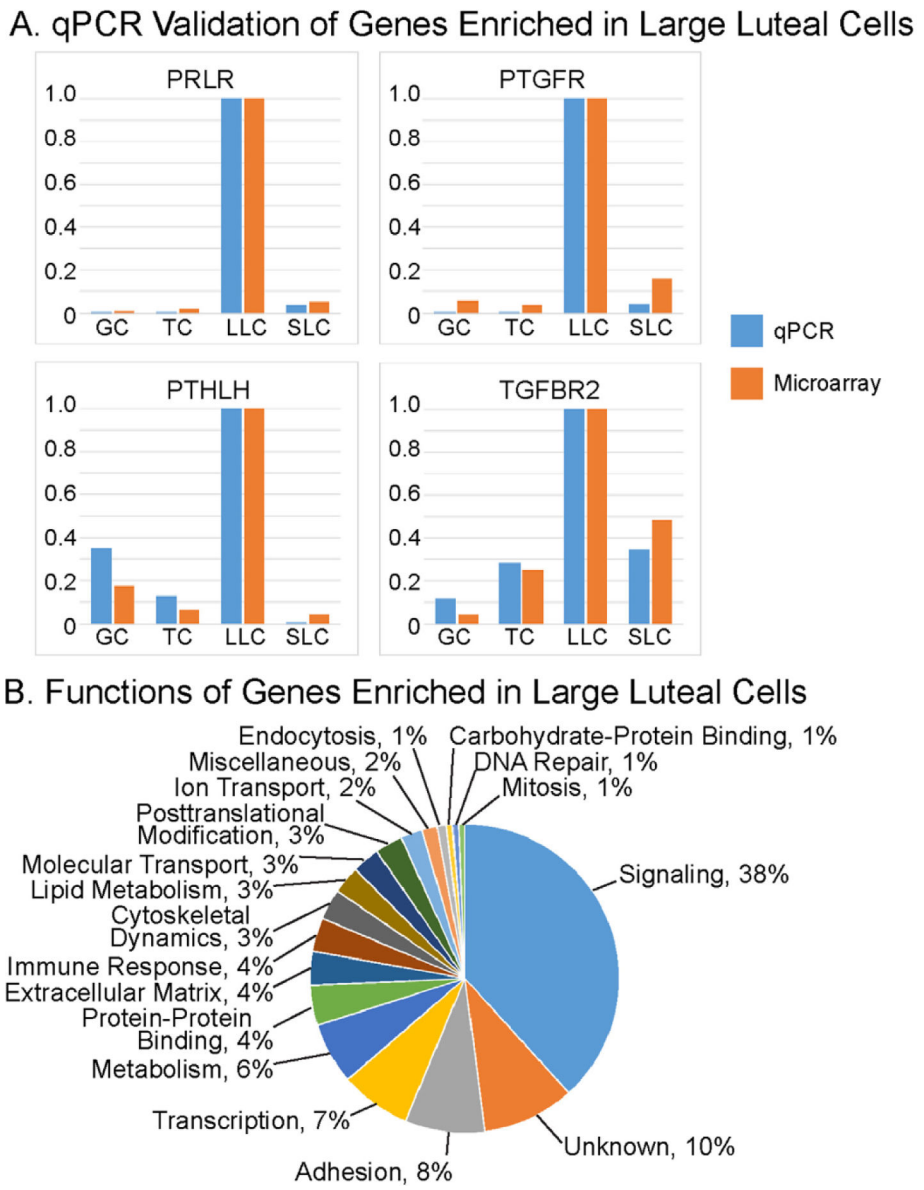

Fig. 4.

Large luteal cell-enriched gene set validation and functional categorization. (A) Validation of select large luteal cell (LLC)-enriched genes with qPCR (blue) compared to the microarray fold changes (orange). (B) Functional categorization of genes enriched in LLC samples shown as a percentage of the 311 differentially regulated transcripts.

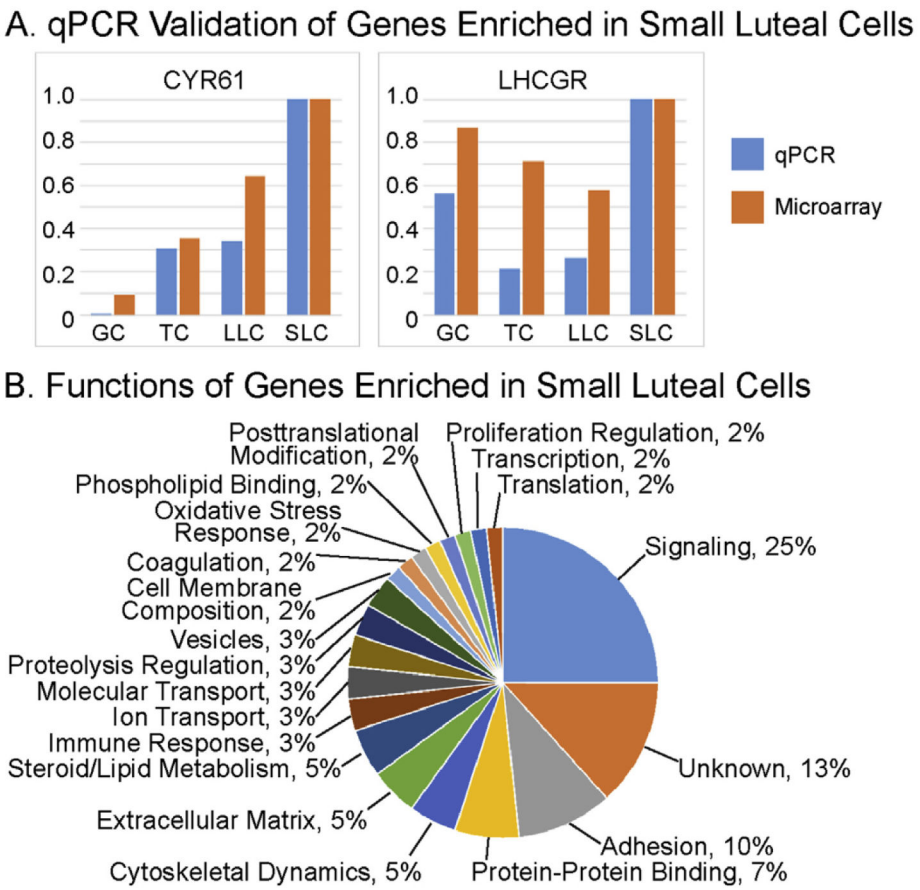

Fig. 5.

Small luteal cell-enriched gene set validation and functional categorization. (A) Validation of select small luteal cell (SLC)-enriched genes with qPCR (blue) compared to the microarray fold changes (orange). (B) Functional categorization of genes enriched in SLC samples shown as a percentage of the 60 differentially regulated transcripts.

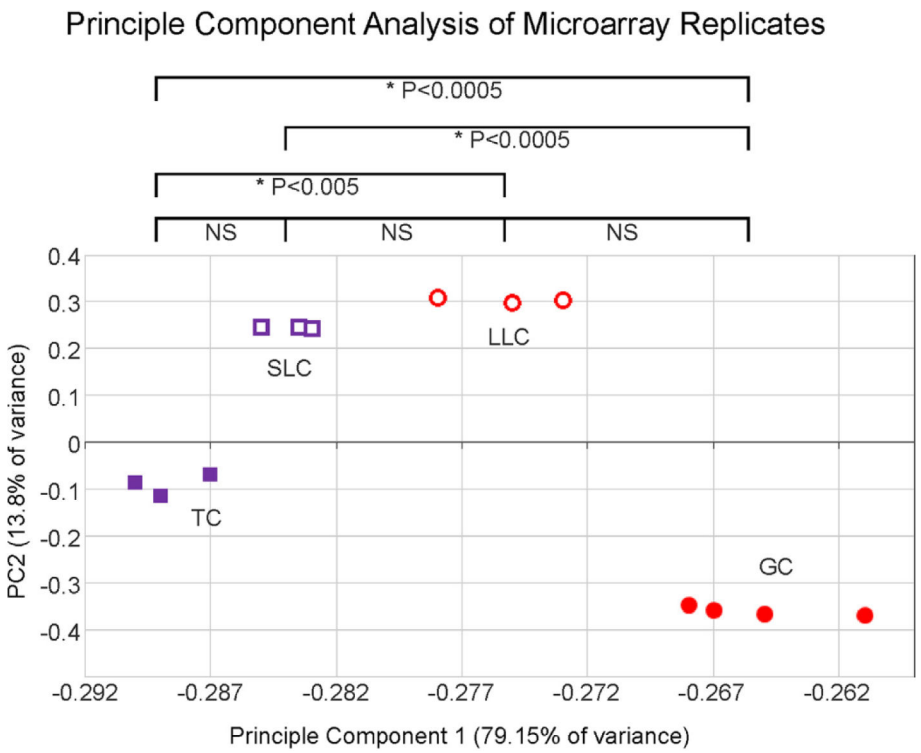

Fig. 6.

Principle Component Analysis of microarray replicates. The gene expression profile data for each microarray was transformed with Principle Component Analysis to visualize relationships between samples and emphasize variation by graphing them in two dimensions based on Principle Component 1 (PC1) and PC2. The individual microarray replicates within a sample type cluster together, and the Eigenvalues for PC1 (x coordinates) indicate that granulosa cells (GC) and large lutea cells (LLC) share gene expression patterns (average PC1 Eigenvalues not significantly different) as do theca cells (TC) and small luteal cells (SLC).

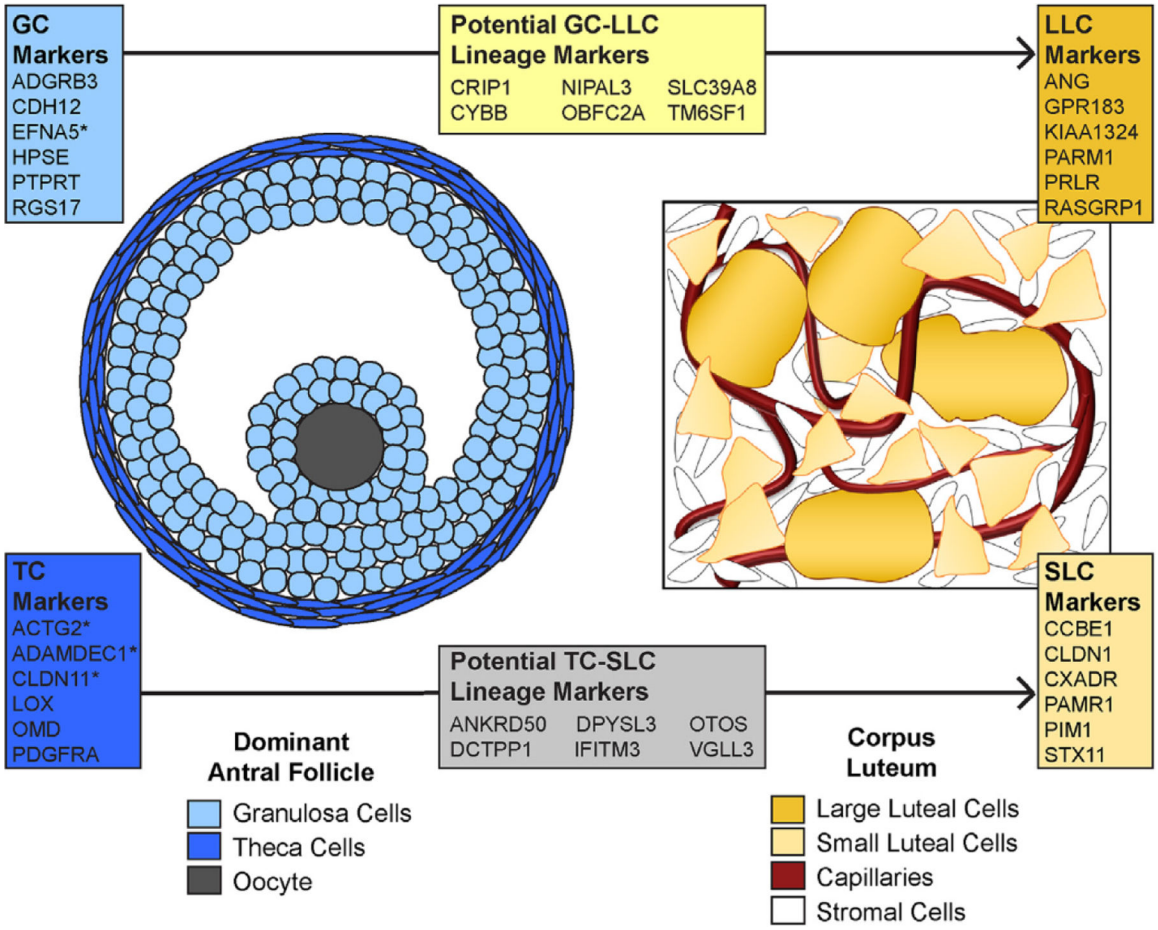

Fig. 7.

Diagram of the expression of the identified cell-type makers and potential lineage markers. The ovarian follicle and the corpus luteum and the major cell types present are illustrated. The expression of the newly identified and canonical (indicated with *) cellular markers are shown along with the potential lineage markers.

Table 1

qPCR Primers.

Primer	Forward	Reverse
ACTG2	GGCTATGCACTGCCTCATGC	ATTTCTCGCTCGGCTGTGGT
CDH12	CCTGTAGGACTTAGCACTGGGG	ACAGCACAACTATGGCTAAGAGT
COL1A2	CGGACTTTGTTGCTGCTTGC	CACTTGGGCCCTTTCTTGCAG
CYP17A1	GACTCCAGCATTGGCGACCT	GGGATGCTGCCACTCCTTCT
CYP19A1	TTCAACAGCAGAGAAGCTGGAA	CCACGTTTCTCAGCAAAAATCA
CYR61	GAAGCGGCTCCCCGTTTTTG	ACGCGTGTGGAGATACCAGT
FSHR	GGGATGCAGTCGAACTGAGGT	TGGGCAGGTTGGAGAACACG
INHBB	ATCAGCTTCGCCGAGACAGATGG	GTAGGGCAGCAGCTTCAGGTA
LHCGR	CTTGCCAACAAACGAGCAAAA	ATCCCAGCCACTCAGTTCAC
LOX	CGTCCGCTGTGAAATTCGCT	TGGCTTGCTTTCTAATACGGTGA
PRLR	TCTGCTGGAGAAGGGCAAGTC	TCAGCAAGTCCTCGCAGTCA
PTGFR	CACAGACAAGGCAGGTCTCA	GGCCATTGTCACCAGAAAAGG
PTHLH	CGGTTATTATTTCGGAGGAGGCG	CCTCTCGCTCTGGGGACTTAT
RPL15	TGGAGAGTATTGCGCCTTCTC	CACAAGTTCCACCACACTATTGG
RPL19	CAGACGATACCGTGAATCTAAGAAGA	TGAGAATCCGCTTGTTTTTGAA
TGFBR2	TCCCAAGTCGGTTAACAGCGA	CCGCACGTCGCAGAACTTAC

Mol Cell Endocrinol. Author manuscript; available in PMC 2019 August 27.

Table 2

Select predicted functions shared among all four cell types.

Category and functional annotation	GC		TC		LLC		SLC	
	p-Value	# RNAs	p-Value	# RNAs	p-Value	# RNAs	p-Value	# RNAs
Cell cycle progression	1.30E-20	511	2.29E-12	469	1.69E-13	485	3.99E-08	452
Cell death	4.32E-23	1450	9.77E-33	1486	2.51E-54	1612	3.59E-40	1546
Cell survival	7.12E-10	589	6.66E-10	583	5.75E-23	664	3.17E-14	619
Expression of RNA	1.29E-18	964	1.65E-19	959	8.89E-29	1027	2.96E-26	1010
Metabolism of protein	1.60E-25	481	5.93E-35	506	2.13E-42	536	1.15E-43	537
Organization of cytoplasm	2.55E-06	652	2.04E-09	670	4.89E-16	111	1.39E-09	683
Proliferation of cells	2.77E-12	1489	1.03E-22	1546	2.27E-47	1704	8.67E-29	1608

Table 3

Cell type-specific markers and potential lineage markers.

Gene symbol	Description	Molecule type	Functional Category	qPCR fold changes			Average linear microarray results (arbitrary units)			
				Fold change (GC vs LLC)	Fold change (GC vs SLC)	Fold change (GC vs TC)	GC	TC	LLC	SLC
Identified GC markers										
ADGRB3	Adhesion G Protein-Coupled Receptor B3 (ADGRB3, BAI3)	Membrane-bound receptor	Signaling	15.77	14.10	6.56	294	48	19	21
CDH12	Cadherin 12, type 2 (N-cadherin 2)	Membrane-bound protein	Adhesion	107.92	166.92	2.75	1446	524	15	9
EFNA5[a]	Ephrin-A5	Membrane-bound protein	Signaling	11.93	25.07	5.41	1224	228	102	50
HPSE	Heparanase	Secreted enzyme	Extracellular matrix	36.72	34.17	7.92	380	47	10	11
PTPRT	PREDICTED: protein tyrosine phosphatase, receptor type, T	Membrane-bound receptor	Signaling	20.76	23.33	12.48	639	65	40	34
RGS17	Regulator of G-protein signaling 17	GTPase activating protein	Signaling	30.27	28.05	5.60	428	75	14	15
Traditional GC markers										
CYP19A1[a]	Cytochrome P450, family 19, subfamily A, polypeptide 1	Intracellular enzyme	Steroidogenesis	63.89	459.93	1.55	6741	4348	106	15
FSHR[a]	Follicle stimulating hormone receptor	Membrane-bound receptor	Signaling	36.19	93.86	3.30	1627	479	47	17
Identified TC markers										
ACTG2[a]	Actin, gamma 2, smooth muscle, enteric	Cytoskeletal component	Cytoskeletal dynamics	10.22	12.67	12.36	157	1866	180	155
ADAMDEC1[a]	ADAM-like, decysin 1	Secreted enzyme	Extracellular matrix remodeling	54.16	30.70	45.45	20	912	18	33
CLDN11[a]	Claudin 11	Membrane-bound protein	Adhesion	20.49	18.27	18.56	63	1203	57	65
LOX	Lysyl oxidase	Secreted enzyme	Extracellular matrix	24.80	13.16	54.30	38	2036	83	160
OMD	Osteomodulin	Secreted proteoglycan	Extracellular matrix	26.21	43.52	47.82	18	865	33	20
PDGFRA	Platelet-derived growth factor receptor, alpha polypeptide	Membrane-bound receptor	Signaling	24.34	15.81	16.01	57	911	37	57
Traditional TC marker										

Gene symbol	Description	Molecule type	Functional Category	qPCR fold changes			Average linear microarray results (arbitrary units)			
				Fold change (GC vs LLC)	Fold change (GC vs SLC)	Fold change (GC vs TC)	GC	TC	LLC	SLC
CYP17A1[a]	Cytochrome P450, subfamily XVII	Intracellular enzyme	Steroidogenesis	11.60	129.71	37.02	112	3859	365	31
Identified LLC markers										
ANG	Angiogenin, ribonuclease, RNase A family, 5	Secreted enzyme	Signaling	118.60	49.11	11.86	12	29	1367	128
GPR183	G protein-coupled receptor 183	Membrane-bound receptor	Signaling	19.22	22.19	25.89	65	56	1341	50
KIAA1324	PREDICTED: K1AA1324 ortholog, transcript variant 1	Intracellular protein	Signaling	32.00	33.17	33.01	26	25	863	25
PARM1	Prostate androgen-regulated mucin-like protein 1	Intracellular protein	Signaling	35.04	19.63	9.64	30	53	1049	110
PRLR	Prolactin Receptor	Membrane-bound receptor	Signaling	91.77	54.49	19.28	15	25	1429	77
RASGRP1	RAS guanyl releasing protein 1 (calcium and DAG-regulated)	Guanine nucleotide exchange factor	Signaling	26.73	25.62	16.58	44	46	1227	77
Traditional LLC marker										
PTGFR	Prostaglandin F receptor (FP)	Membrane-bound receptor	Signaling	16.12	27.63	6.38	436	248	6606	1056
Identified SLC markers										
CCBE1	Collagen And Calcium Binding EGF Domains 1	Intracellular protein	Extracellular matrix remodeling	27.13	14.20	3.75	37	69	267	1024
CLDN1	Claudin 1	Membrane-bound protein	Adhesion	9.64	4.50	2.69	50	100	167	448
CXADR	Coxsackie virus and adenovirus receptor	Membrane-bound receptor	Cell-cell adhesion	8.99	3.32	2.16	97	267	404	878
PAMR1	Peptidase domain containing associated with muscle regeneration 1	Intracellular protein	Unknown	24.97	23.30	3.09	27	28	224	669
PIM1	Pim-1 Proto-Oncogene, Serine/ Threonine Kinase	Intracellular kinase	Signal transduction	7.65	6.04	2.52	85	107	251	651
STX11	Syntaxin 11	Vesicle-localized protein	Intracellular transport	11.59	13.76	2.69	52	43	222	616
Traditional SLC marker										
LHCGR	Luteinizing hormone receptor	Membrane-bound receptor	Signal transduction	1.15	1.40	1.73	3117	2830	2292	3974

Gene symbol	Description	Molecule type	Functional Category	qPCR fold changes			Average linear microarray results (arbitrary units)			
				Fold change (GC vs LLC)	Fold change (GC vs SLC)	Fold change (GC vs TC)	GC	TC	LLC	SLC
Potential lineage markers (GC- > LLC)										
CRIP1	Cysteine-Rich Protein 1	Intracellular protein	Protein-protein binding				494	25S	659	15S
CYBB	Cytochrome B-245, Beta Polypeptide	Transmembrane enzyme	Ion transport				600	363	831	35
NIPAL3	NIPA-Like Domain Containing 3	Transmembrane protein	Molecular transport				822	432	672	319
OBFC2A	Nucleic Acid Binding Protein 1 (NABP1, OBFC2A)	DNA-binding protein complex subunit	DNA repair				1286	347	697	217
SLC39A8	Solute Carrier Family 39 (Zinc Transporter), Member 8	Transmembrane protein	Ion transport				1191	291	741	375
TM6SF1	Transmembrane 6 Superfamily Member 1	Transmembrane protein	Lysosomal function				757	361	793	149
Potential lineage markers (TC- > SLC)										
ANKRD50	Ankyrin repeat domain 50	Intracellular protein	Protein trafficking				313	1127	468	920
DCTPP1	DCTP Pyrophosphatase 1	Intracellular enzyme	Metabolism				363	1814	526	1216
DPYSL3	Dihydropyrimidinase-like 3	Intracellular protein	Signaling				42	540	231	508
IFITM3	Interferon induced transmembrane protein 3	Transmembrane protein	Signaling				215	890	365	598
OTOS	Otospiralin	Transmembrane protein	Signaling				43	3338	354	1317
VGLL3	Vestigial like 3	Transcriptional coactivator	Transcription				85	498	195	696

[a] Also identified in other published microarray analyses.

Table 4

Predicted functional consequences of the granulosa cell transcriptome.

Category and functional annotation	p-Value	# RNAs
Select predicted functional consequences of the entire* CC *transcriptome		
Assembly of protein-protein complex	1.17E-04	85
Colony formation of cells	2.55E-04	200
Decay of RNA	7.31E-05	18
G2 phase	4.36E-08	126
Morphology of clathrin-coated structures	2.64E-04	33
Phosphorylation of protein	1.93E-04	292
Repression of RNA	2.99E-04	77
S phase	8.29E-11	131
Small GTPase mediated signal transduction	1.53E-04	81
Predicted functional consequences of the genes enriched/decreased* in *CCs vs. TCs, LLCs, and SLCs		
Select granulosa cell functions with increased predicted activation state (z-score >2)		
Alignment of chromosomes	2.97E-12	12
Cell survival	1.51E-04	78
Cycling of centrosome	3.34E-07	14
Formation of microtubules	2.83E-03	8
Growth of connective tissue	9.88E-08	53
Invasion of cells	1.54E-04	51
Metabolism of DNA	1.07E-08	40
Proliferation of cells	4.25E-06	187
Repair of cells	9.93E-04	9
Repair of DNA	3.14E-05	25
Synthesis of DNA	7.90E-10	42
Select granulosa cell functions with decreased predicted activation state (z-score < −7)		
Aneuploidy	9.89E-05	10
Cell death	2.06E-07	180
DNA damage	1.41E-06	21
Formation of mitotic spindle	5.17E-07	12
Fragmentation of nucleus	9.31E-04	6

Table 5

Predicted functional consequences of the theca cell transcriptome.

Category and functional annotation	p-Value	# RNAs
Select predicted functional consequences of the entire TC transcriptome		
Aerobic respiration of cells	1.90E-04	14
Glycolysis of cells	1.62E-04	50
Growth of ovarian follicle	3.41E-05	29
Insulin-like growth factor receptor signaling pathway	1.89E-04	11
Metabolism of heme	1.61 E-04	10
Oxidation of protein	1.75E-06	19
Synthesis of carbohydrate	1.40E-04	182
Synthesis of sterol	4.14E-05	39
Tetramerization of protein	7.83E-06	56
Predicted functional consequences of the genes enriched/decreased in TCs* vs. *GCs, LLCs, and SLCs		
Select theca cell functions with increased predicted activation state (z-score >2)		
Development of urinary tract	1.91E-03	9
Formation of kidney	5.81E-03	8
Migration of cells	1.31E-02	30
Select theca cell functions with decreased predicted activation state (z-score < −2)		
Aortic disorder	2.95E-03	6
Congenital anomaly of musculoskeletal system	6.29E-06	21
Hypoplasia of thorax	7.81E-03	6

Table 6

Predicted functional consequences of the genes enriched/decreased in follicular cells.

Category and functional annotation	p-Value	# RNAs
Select follicular cell functions with increased predicted activation state (z-score >2)		
Cell Cycle: cell cycle progression	3.05E-34	163
Cell Cycle: M phase	6.40E-17	48
Cell Cycle: interphase	7.58E-15	87
Cell Cycle: S phase	3.70E-11	41
Cell Cycle: G1/S phase transition	1.06E-05	26
Cell Cycle: cytokinesis	6.49E-09	30
Cell Death and Survival: cell survival	3.38E-09	131
Cellular Organization: organization of cytoplasm	2.16E-07	134
Cellular Organization: organization of cytoskeleton	2.30E-07	124
Cellular Organization: microtubule dynamics	3.20E-07	108
Cellular Proliferation: proliferation of cells	1.53E-11	301
DNA Replication and Repair: checkpoint control	1.27E-11	24
DNA Replication and Repair: metabolism of DNA	5.46E-19	69
DNA Replication and Repair: DNA replication	5.84E-15	46
DNA Replication and Repair: repair of DNA	7.87E-13	47
DNA Replication and Repair: recombination	1.16E-10	33
DNA Replication and Repair: excision repair	1.83E-06	15
DNA Replication and Repair: degradation of DNA	9.83E-05	22
Gene Expression: transcription of RNA	1.60E-04	142
Post-Translational Modification: phosphorylation of protein	2.20E-06	71
Reproductive System Function: ovulation	2.23E-05	13
Reproductive System Function: entry into interphase of oocytes	2.88E-06	4
Small Molecule Biochemistry: hydrolysis of ATP	1.31E-04	9
Small Molecule Biochemistry: hydrolysis of nucleotide	3.43E-05	17
Tissue Development: growth of connective tissue	1.94E-06	64
Select follicular cell functions with decreased predicted activation state (z-score < 2)		
Cell Cycle: aneuploidy	3.82E-06	14

Category and functional annotation	p-Value	# RNAs
Cell Death and Survival: cell death	3.45E-12	280
Cell Death and Survival: apoptosis	7.60E-12	231
Cell Death and Survival: necrosis	7.41E-11	222
Reproductive System Disease: hyperplasia of gonad	3.67E-06	16

Table 7

Predicted functional consequences of the large luteal cell transcriptome.

Category and functional annotation	p-Value	# RNAs
Select *predicted functional consequences of the entire LLC transcriptome*		
Binding of cells	7.00E-06	201
Branching of cells	2.63E-08	183
Cellular homeostasis	6.06E-10	702
Development of blood cells	2.11E-07	319
Growth of epithelial tissue	1.02E-07	309
Microtubule dynamics	4.86E-08	532
Production of reactive oxygen species	6.91E-06	159
Quantity of connective tissue	2.74E-06	269
Transport of molecule	1.20E-07	701
Predicted functional consequences of the genes enriched/decreased in LLCs vs. CCs, TCs, and SLCs		
Select large luteal cell functions with increased predicted activation stale (z-score >2)		
Activation of cells	8.92E-11	52
Angiogenesis	5.85E-31	82
Cell cycle progression	2.64E-04	39
Cell movement	6.82E-25	116
Cell survival	1.36E-11	68
Cellular homeostasis	2.28E-07	63
Chemotaxis	1.16E-11	38
Development of cytoplasm	8.97E-05	23
Differentiation of cells	6.62E-16	104
Endocytosis	2.19E-05	20
Formation of cytoskeleton	8.03E-05	20
Inflammatory response	1.23E-13	50
Ion homeostasis of cells	3.73E-05	27
Maturation of cells	2.60E-07	27
Migration of cells	4.60E-26	111
Migration of endothelial cells	1.51E-14	33
Proliferation of cells	1.79E-17	146
Quantity of Ca2+	8.67E-06	23
Quantity of metal ion	4.13E-06	25
Synthesis of DNA	8.06E-07	25
Synthesis of lipid	5.28E-06	35
Transport of ion	8.11E-05	24
Select large luteal cell functions with decreased predicted activation state (z-score <−2)		
Apoptosis	1.38E-11	106
Cell death	5.33E-12	125
Glucose metabolism disorder	1.18E-05	47

Table 8

Predicted functional consequences of the small luteal cell transcriptome.

Category and functional annotation	**p-Value**	**# RNAs**
Select predicted functional consequences of the entire SLC transcriptome		
Metabolism of phospholipid	2.78E-06	109
Metabolism of peptide	1.48E-05	86
Dephosphorylation of protein	1.01E-04	71
Migration of epithelial cells	3.16E-05	57
Concentration of ATP	1.09E-04	55
Metabolism of sterol	1.64E-05	52
Formation of cellular inclusion bodies	4.53E-05	43
Oxidative stress response of cells	5.51E-06	33
Pinocytosis	7.39E-05	19
Predicted functional consequences of the genes enriched/decreased in SLCs* vs. *GCs, TCs, and LLCs		
Select small luteal cell functions with increased predicted activation state (z-score >2)		
Category and Functional Annotation	p-Value	# RNAs
Aggregation of blood platelets	8.36E-04	5
Cancer	2.13E-03	54

Table 9

Predicted functional consequences of the genes enriched/decreased in luteal cells.

Category and functional annotation	p-Value	# RNAs
Select luteal cell functions with increased predicted activation state (z-score > 2)		
Carbohydrate Metabolism: metabolism of carbohydrate	3.34E-13	87
Cardiovascular System: angiogenesis	2.92E-33	159
Cardiovascular System: migration of endothelial cells	1.4E-14	58
Cell Cycle: interphase	8.39E-14	92
Cell Death and Survival: cell survival	2.74E-28	199
Cell Morphology: formation of cellular protrusions	2.91E-11	109
Cell-mediated Immune Response: T cell development	3.27E-16	81
Cell-To-Cell Interaction: activation of cells	4.09E-22	144
Cell-To-Cell Interaction: adhesion of blood cells	7.41 E-16	66
Cell-To-Cell Interaction: adhesion of connective tissue	6.35E-12	33
Cell-To-Cell Interaction: 1-kappaB kinase/NF-kappaB cascade	1.13E-10	33
Cell-To-Cell Interaction: protein kinase cascade	3.19E-13	66
Cell-To-Cell Interaction: recruitment of immune cells	3.12E-17	66
Cellular Organization: organization of cytoplasm	4.33E-16	180
Cellular Organization: organization of cytoskeleton	8.3E-16	167
Cellular Development: differentiation of cells	3.73E-29	280
Cellular Development: maturation of cells	2.45E-09	61
Cellular Function and Maintenance: cellular homeostasis	4.84E-26	206
Cellular Growth: development of blood cells	5.66E-18	101
Cellular Growth: differentiation of connective tissue	3.24E-20	114
Cellular Growth: proliferation of cells	1.63E-45	442
Cellular Movement: cell movement	2.59E-42	300
Cellular Movement: migration of cells	3.49E-38	270
DNA Replication: synthesis of DNA	5.59E-15	69
Free Radicals: metabolism of reactive oxygen species	1.78E-13	75
Gene Expression: transcription	5.84E-21	235
Inflammatory Response: immune response of cells	2.23E-16	89

Category and functional annotation	p-Value	# RNAs
Inflammatory Response: inflammatory response	1.24E-28	136
Lipid Metabolism: biosynthesis of fatty acids	1.61E-09	37
Lipid Metabolism: fatty acid metabolism	2.78E-20	100
Lipid Metabolism: metabolism of cholesterol	1.26E-12	27
Lipid Metabolism: metabolism of eicosanoid	1.67E-09	39
Lipid Metabolism: metabolism of membrane lipid	2.2E-17	70
Lipid Metabolism: metabolism of sterol	7.34E-13	28
Lipid Metabolism: metabolism of terpenoid	9.32E-14	53
Lipid Metabolism: steroid metabolism	6.41E-14	48
Lipid Metabolism: synthesis of fatty acid	4.15E-15	57
Lipid Metabolism: synthesis of lipid	5.81E-30	131
Lipid Metabolism: synthesis of steroid	7.09E-12	45
Lipid Metabolism: synthesis of terpenoid	7.05E-11	46
Molecular Transport: transport of molecule	9.62E-18	192
Post-Translational Modification: phosphorylation of protein	3.78E-11	93
Reproductive System Function: fertility	1.9E-10	54
Reproductive System Function: quantity of gonad	3.74E-10	37
Tissue Development: growth of connective tissue	2.1E-18	101
Tissue Morphology: quantity of cells	6.59E-35	250
Select luleal cell functions with decreased predicted activation state (z-score < −2)		
Cell Death and Survival: cell death	3.48E-42	405
Inflammatory Response: inflammation of organ	9.34E-31	183
Metabolic Disease: glucose metabolism disorder	2.48E-14	153